Cell Reports, Volume *22*

Supplemental Information

Mechanistic Differences in Neuropathic Pain Modalities Revealed by Correlating Behavior with Global Expression Profiling

Enrique J. Cobos, Chelsea A. Nickerson, Fuying Gao, Vijayendran Chandran, Inmaculada Bravo-Caparrós, Rafael González-Cano, Priscilla Riva, Nick A. Andrews, Alban Latremoliere, Corey R. Seehus, Gloria Perazzoli, Francisco R. Nieto, Nicole Joller, Michio W. Painter, Chi Him Eddie Ma, Takao Omura, Elissa J. Chesler, Daniel H. Geschwind, Giovanni Coppola, Manu Rangachari, Clifford J. Woolf, and Michael Costigan

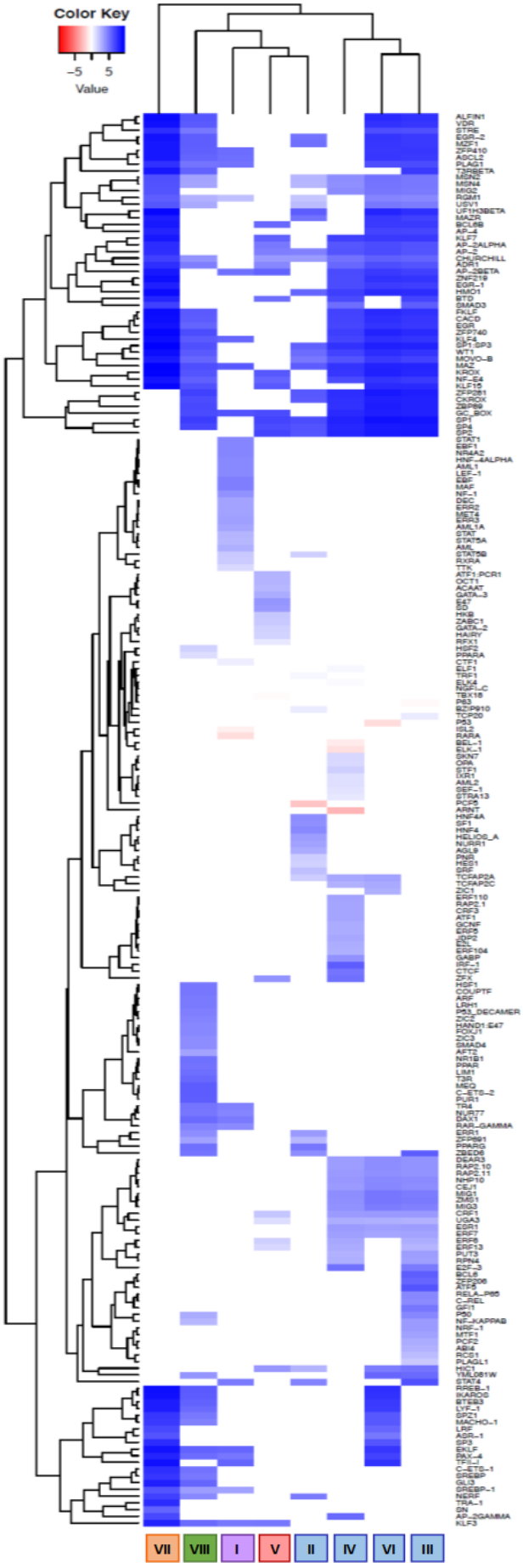

Figure S1 (Related to Figure 3). Transcription factor binding-site (TFBS) enrichment in each injury associated module. Heat map of 210 TFs (right margin) whose DNA-binding motifs were over-represented in the promoters of at least one gene cluster. Log-transformed raw enrichment score from clover algorithm was utilized for hierarchical clustering (Table S2). Hierarchical clustering of TFBS enrichment score for each cluster demonstrated the separation of neuronal and immune associated gene modules. Color code for gene clusters: Neuronal – Blue; Immune – Orange; Mixed – Green; Chemotaxis – Purple; Unknown – Red.

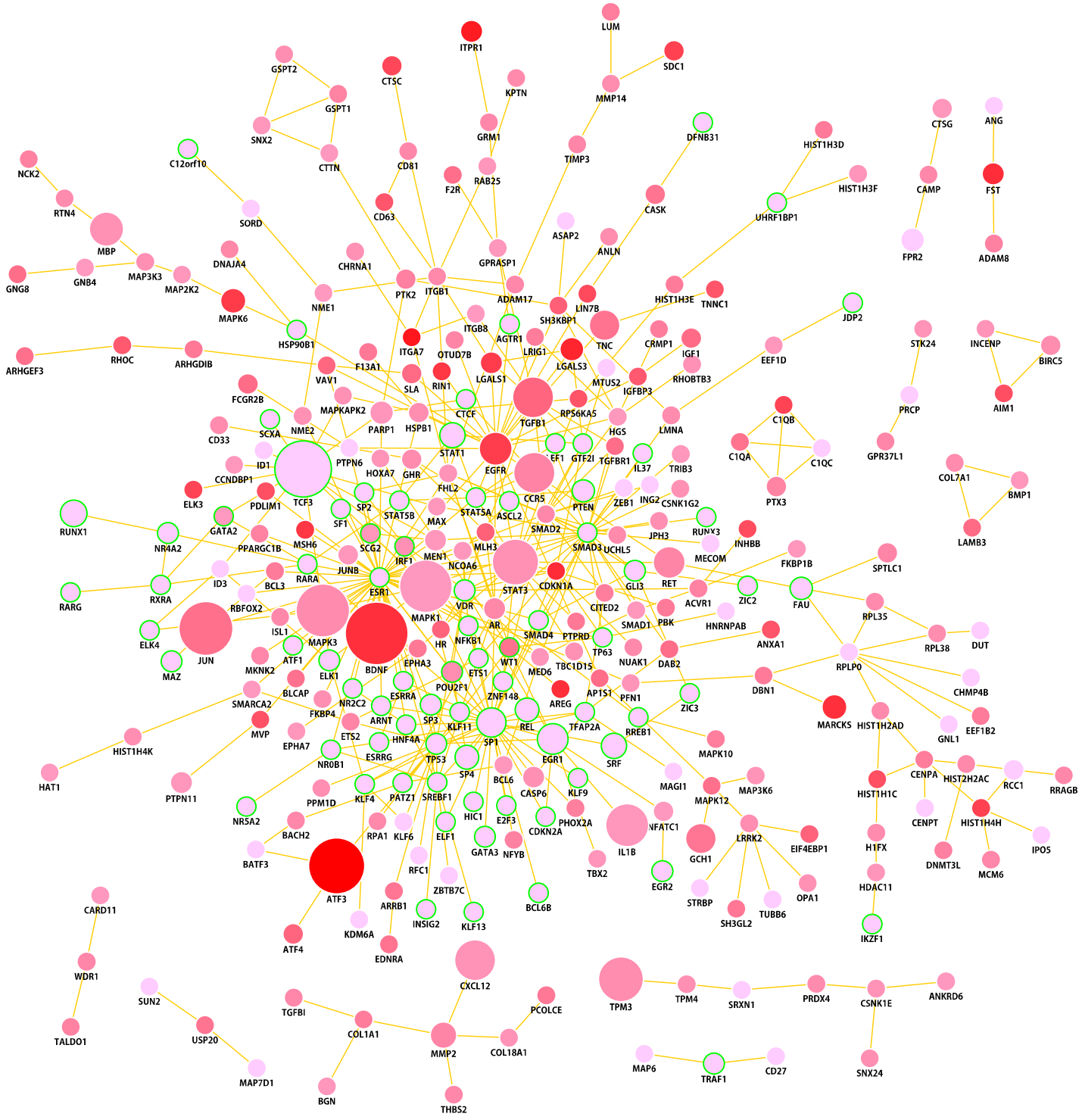

Figure S2 (Related to Figure 3). Protein-protein interaction network of genes differentially expressed in the DRG up to 10 post SNI nerve injury. Nodes correspond to genes and edges to protein-protein interaction (PPI). Over-represented TFs are encircled in green. Larger nodes correspond to number of PubMed hits with co-occurrence of gene and tactile allodynia, cold allodynia, neuropathic sensitivity or neuropathic pain tags. Nodes are colored based on their F-statistic values, pink to red (low to high).

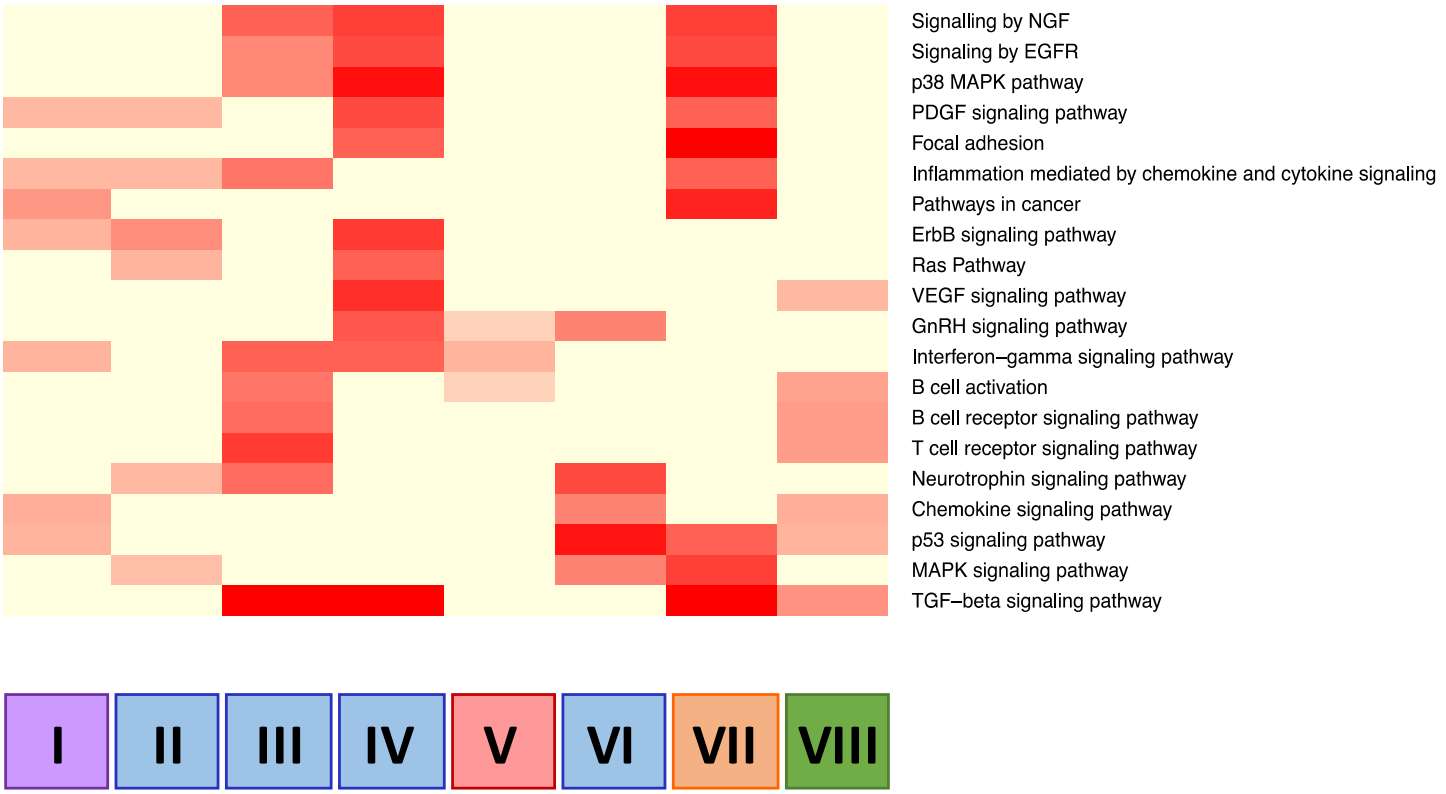

Figure S3 (Related to Figure 3). Signaling pathway enrichment analyses of neuropathic pain associated clusters. Heat map of twenty enriched pathways (Benjamini-corrected P-values < 0.05) in the PPI network and their association with eight neuropathic pain associated clusters are shown. Heat map are color-coded based on the percentage of individual pathway genes present in the corresponding neuropathic pain associated clusters (red is higher). Color code for gene clusters: Neuronal – Blue; Immune – Orange; Mixed – Green; Chemotaxis – Purple; Unknown –Red.

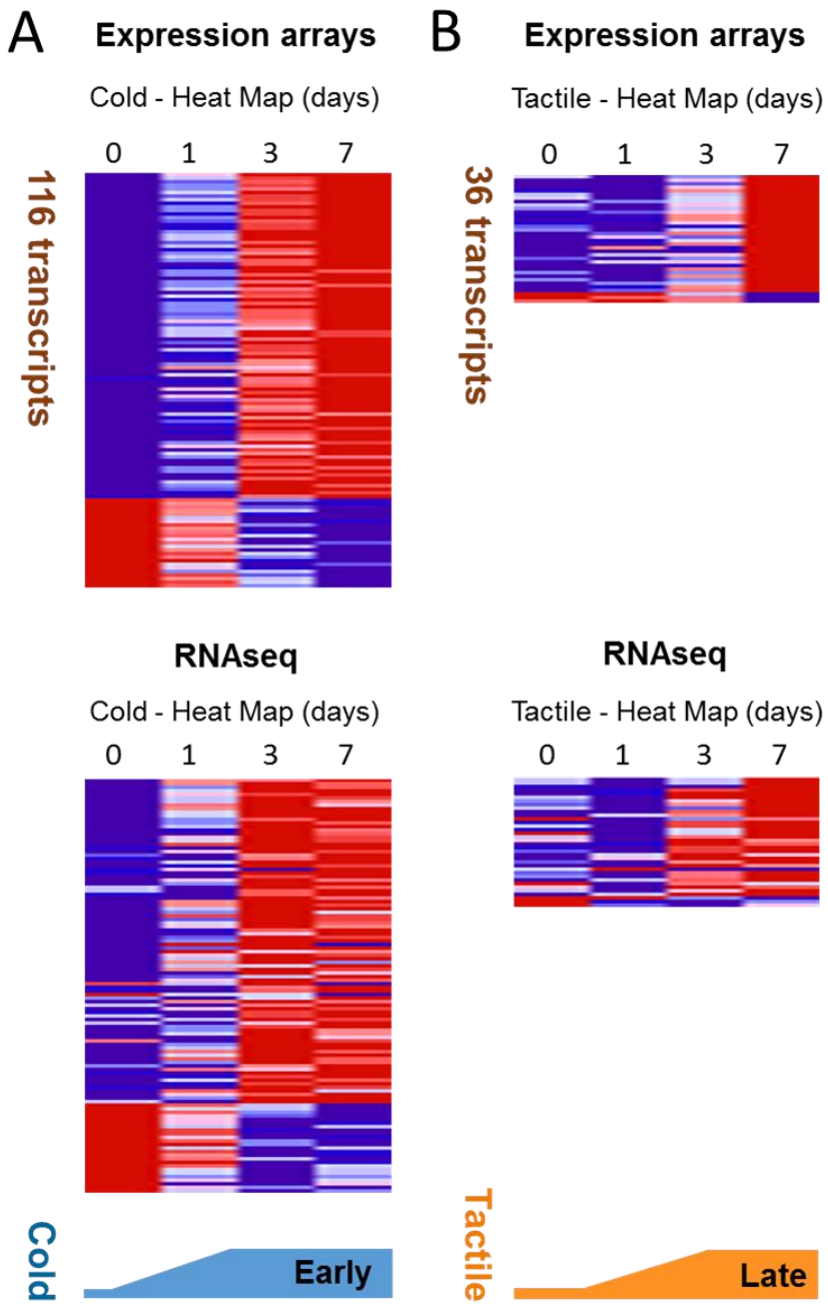

Figure S4 (Related to Figure 4). Expression heat maps of transcripts across four time points (Naïve, 1, 3, and 7 days post SNI). Common genes between the expression arrays and RNAseq data in each sensory modality (Cold and Tactile) are shown. These data demonstrate that the overall expression patterns of the constituent genes of each modality group were virtually identical regardless of the platform used to define the genes regulation. These data therefore act as a biological replicate of the expression groups used. The RNAseq data, as a whole, acts as a biological replicate of the entire data set. Heat map are color-coded based on the relative expression of individual transcripts (blue lower red higher expression). Color code for gene clusters: Cold – Blue; Immune – Orange.

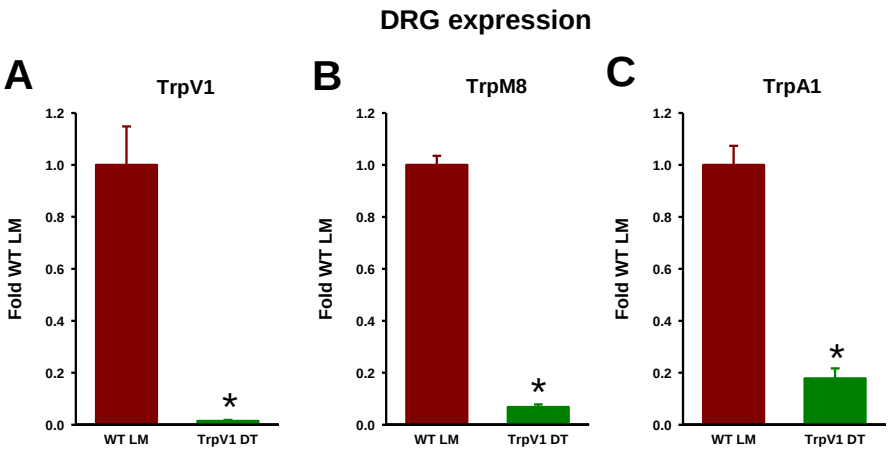

Figure S5 (Related to Figure 5). Expression of TrpV1, TrpM8 and TrpA1 in the DRG, determined by quantitative real-time PCR, from mice lacking TrpV1-lineage nociceptors (TrpV1 DTA) and in their wild-type littermate controls (WT LM). **(a)** TrpV1, **(b)** TrpM8 and **(c)** TrpA1 expression. Statistically significant differences between the values from both genotypes: **p<0.01 (unpaired Student's t-test). In all panels error bars indicate SEM.

Table S1 (Related to Figure 2). WGCNA analysis of all regulated transcripts in DRG. Significantly regulated probes across 10 days post SNI ($p<0.01$; moderated F-statistic, n=1704) were subject to WGCNA analysis to produce clusters of co-regulated transcripts, with no preconceived structure.

This table is provided as an Excel file.

Table S2 (Related to Figure 3). Analysis of transcription factor binding-sites (TFBS) enrichment. For estimation of TFBSs enrichment in the identified corresponding cluster-genelist promoter sequences (1000bp upstream from transcription start site), p-values were obtained relative to three background datasets: 1000bp of sequence upstream of all mouse gene, mouse CpG islands and mouse chromosome 19. Enriched TFBS position weight matrices from both JASPAR and TRANSFAC databases are provided in this table along with their clover enrichment score for each clusters.

This table is provided as an Excel file.

Table S3 (Related to Figure 3). Pathway analysis of the protein-protein interaction network from neuropathic pain associated clusters. For categorization and clustering of signaling pathway, we considered pathway terms with Benjamini-corrected p-values less than 0.05. The gene names and total number of genes present in each pathway are provided.

This table is provided as an Excel file.

Table S4 (Related to Figure 4). Correlation of the time course of neuropathic cold allodynia with transcript regulation in the DRG post SNI. The table shows the Pearson correlation coefficient as a measure of the degree of linear dependence between transcript regulation and sensory hypersensitivity. This parameter ranges from -1 (complete inverse correlation) through zero (no correlation) to 1 (maximal direct correlation). Probes are classified as up or downregulated based on the direct or inverse correlation with the increased neuropathic cold sensitivity. Absolute Pearson correlation indicates the absolute value of this parameter. Only those probes with an overall $p<0.01$ across the time course (moderated F-statistic) and an absolute Pearson correlation coefficient > 0.75 are shown.

This table is provided as an Excel file.

Table S5 (Related to Figure 4). Correlation of the time course of neuropathic tactile allodynia with transcript regulation in the DRG post SNI. The table shows the Pearson correlation coefficient as a measure of the degree of linear dependence between transcript regulation and sensory hypersensitivity. This parameter ranges from -1 (complete inverse correlation) through zero (no correlation) to 1 (maximal direct correlation). Probes are classified as down or upregulated based on the direct or inverse correlation with the decreased mechanical threshold during neuropathy. Absolute Pearson correlation indicates the absolute value of this parameter. Only those probes with an overall $p<0.01$ across the time course (moderated F-statistic) and an absolute Pearson correlation coefficient > 0.75 are shown.

This table is provided as an Excel file.

Table S6 (Related to Figure 4). Functional enrichment analysis using Ingenuity Pathway Analysis (IPA) software of the genes whose expression in the DRG correlates with neuropathic cold allodynia. Table shows selected functional annotations and their gene content. Analysis was performed on probes with an overall $p<0.01$ across the time course (moderated F-statistic) and an absolute Pearson correlation coefficient > 0.85.

Category	Function	Function Annotation	p-value	Genes
Neurological Disease	seizure disorder	seizure disorder	5.61E-05	AP1S1, C1QB, CA3, CACNA2D1, CITED2, GABRG1, GAL, ITPR1, NNAT, NPY, SCN4B, SLC6A4
Neurological Disease	ischemic stroke	ischemic stroke	2.29E-04	HIST2H2AA3/HIST2H2AA4, SLC6A4, VSNL1, XDH
Neurological Disease	Migraines	Migraines	3.15E-04	CA3, CACNA2D1, CX3CR1, GABRG1, SCN4B, SLC6A4
Neurological Disease	neuropathic pain	neuropathic pain	1.04E-03	CACNA2D1, KCNS1, SLC6A4

Table S7 (Related to Figure 4). Functional enrichment analysis using Ingenuity Pathway Analysis (IPA) software of the genes whose expression in the DRG correlates with neuropathic tactile allodynia. Table shows selected functional annotations and their gene content. Analysis was performed on probes with an overall $p<0.01$ across the time course (moderated F-statistic) and an absolute Pearson correlation coefficient > 0.85.

Category	**Function**	**Function Annotation**	**p-value**	**Genes**
Immunological Disease	systemic autoimmune syndrome	systemic autoimmune syndrome	1.06E-12	AIF1, C1QA, CCL4, CD74, CTSA, CX3CR1, CXCL16, HLA-DQB1, HLA-DRB5, LGALS1, LY6E, LYZ, MS4A7, RARRES2, TGFBI, TLR2, TYROBP
Cell-To-Cell Signaling and Interaction	activation	activation of antigen presenting cells	5.89E-11	CD74, CSF1R, CTSH, CX3CR1, HLA-DQB1, RARRES2, SLC11A1, TLR2, TREM2, TYROBP
Endocrine System Disorders	Diabetes - type 2	diabetes - type 2	7.86E-11	AIF1, CCL4, CD74, CX3CR1, CXCL16, HLA-DQB1, HLA-DRB5, LYZ, TGFBI, TLR2, TYROBP
Connective Tissue Disorders	rheumatoid arthritis	rheumatoid arthritis	1.82E-08	C1QA, CCL4, CD74, CXCL16, HLA-DQB1, HLA-DRB5, LGALS1, LYZ, MS4A7, RARRES2, TLR2

Table S8 (Related to Figure 4). Functional enrichment analysis using Gene Ontology (GO) software of the genes whose expression in the DRG correlates with neuropathic cold allodynia. Table shows selected functional annotations (GO terms) and their gene content. Analysis was performed on probes with an overall p<0.01 across the time course (moderated F-statistic) and an absolute Pearson correlation coefficient > 0.75.

Sno	Annotation	GO Terms	Count	%	p-value	Genes	List Total	Pop Hits	Pop Total	Fold Enrichment	Bonferroni	Benjamini	FDR
1	GOTERM_MF_FAT	GO:0042165~neurotransmitter binding	11	4.015	6.65E-07	GPR83, GABRG1, GABRG2, GLRB, CCKBR, CHRNA5, PROKR2, HTR3A, CHRNA1, HTR3B, NTSR2	200	87	13288	8.400	2.65E-04	2.65E-04	9.28E-04
2	GOTERM_MF_FAT	GO:0030594~neurotransmitter receptor activity	11	4.015	6.65E-07	GPR83, GABRG1, GABRG2, GLRB, CCKBR, CHRNA5, PROKR2, HTR3A, CHRNA1, HTR3B, NTSR2	200	87	13288	8.400	2.65E-04	2.65E-04	9.28E-04
3	GOTERM_CC_FAT	GO:0045202~synapse	19	6.934	1.06E-05	GABRG1, GABRG2, ACHE, GLRB, CPLX2, LIN7B, CASK, ITPR1, SEMA4F, CHRNA5, SV2B, LGI3, VAMP1, HTR3A, DOC2B, CHRNA1, HTR3B, GAP43, FAIM2	217	319	12504	3.432	0.0026	8.68E-04	0.0138
4	GOTERM_CC_FAT	GO:0044456~synapse part	14	5.109	7.99E-05	GABRG1, GABRG2, GLRB, LIN7B, ITPR1, SEMA4F, CHRNA5, LGI3, SV2B, CHRNA1, HTR3A, DOC2B, HTR3B, FAIM2	217	212	12504	3.805	0.0194	0.0049	0.1034
5	GOTERM_CC_FAT	GO:0045211~postsynaptic membrane	10	3.650	3.33E-04	GABRG1, GABRG2, GLRB, SEMA4F, CHRNA5, LIN7B, HTR3A, CHRNA1, HTR3B, FAIM2	217	126	12504	4.573	0.0783	0.0162	0.4301
6	GOTERM_MF_FAT	GO:0005230~extracellular ligand-gated ion channel activity	7	2.555	4.50E-04	GABRG1, GABRG2, GLRB, CHRNA5, HTR3A, CHRNA1, HTR3B	200	66	13288	7.047	0.1645	0.0353	0.6262
7	GOTERM_MF_FAT	GO:0015267~channel activity	16	5.839	3.98E-04	GABRG1, GABRG2, CACNA2D1, GLRB, AQP9, KCNK1, KCNIP1, ITPR1, FXYD7, KCNIP3, KCNS1, CHRNA5, SCN4B, HTR3A, CHRNA1, HTR3B	200	365	13288	2.912	0.1468	0.0389	0.5532
8	GOTERM_MF_FAT	GO:0022803~passive transmembrane transporter activity	16	5.839	3.98E-04	GABRG1, GABRG2, CACNA2D1, GLRB, AQP9, KCNK1, KCNIP1, ITPR1, FXYD7, KCNIP3, KCNS1, CHRNA5, SCN4B, HTR3A, CHRNA1, HTR3B	200	365	13288	2.912	0.1468	0.0389	0.5532
9	GOTERM_MF_FAT	GO:0005216~ion channel activity	15	5.474	7.90E-04	GABRG1, GABRG2, GLRB, CACNA2D1, KCNK1, KCNIP1, ITPR1, FXYD7, KCNIP3, KCNS1, CHRNA5, SCN4B, HTR3A, CHRNA1, HTR3B	200	349	13288	2.856	0.2703	0.0440	1.0954
10	GOTERM_MF_FAT	GO:0022838~substrate specific channel activity	16	5.839	3.48E-04	GABRG1, GABRG2, CACNA2D1, GLRB, AQP9, KCNK1, KCNIP1, ITPR1, FXYD7, KCNIP3, KCNS1, CHRNA5, SCN4B, HTR3A, CHRNA1, HTR3B	200	360	13288	2.953	0.1297	0.0452	0.4841

Table S9 (Related to Figure 4). Functional enrichment analysis using Gene Ontology (GO) software of the genes whose expression in the DRG correlates with neuropathic tactile allodynia. Table shows selected functional annotations (GO terms) and their gene content. Analysis was performed on probes with an overall p<0.01 across the time course (moderated F-statistic) and an absolute Pearson correlation coefficient > 0.75.

Sno	Annotation	GO Terms	Count	%	p-value	Genes	List Total	Pop Hits	Pop Total	Fold Enrichment	Bonferroni	Benjamini	FDR
1	GOTERM_BP_FAT	GO:0006955~immune response	18	18.750	6.54E-10	TLR2, VTN, H2-AB1, CCL4, TLR7, CLEC4N, RAET1B, TGFB1, FCGR3, C1QA, C1QB, SLC11A1, CXCL14, P2RY14, H2-EB1, CX3CR1, FCER1G, CD14	77	471	13588	6.744	7.22E-07	7.22E-07	8.15E-04
2	GOTERM_CC_FAT	GO:0005576~extracellular region	30	31.250	6.91E-07	GALNT2, RARRES2, CD109, VTN, CCL4, TGFB1, COL7A1, COMP, TGFBI, NMS, LOXL2, PLTP, VNN3, TNXB, LGALS1, MUP3, IGF1, F9, MMP14, C1QA, C1QB, BGN, NPY, CXCL14, NTS, CXCL16, LIPH, NPPB, COL1A1, TREM2	85	1680	12504	2.627	9.61E-05	9.61E-05	1.05E-06
3	GOTERM_BP_FAT	GO:0006954~inflammatory response	11	11.458	4.66E-07	C1QA, C1QB, SLC11A1, TLR2, NPPB, CCL4, TLR7, CD14, TGFB1, F2R, FCGR3	77	225	13588	8.627	5.1413E-04	2.57E-04	0.0007
4	GOTERM_CC_FAT	GO:0044421~extracellular region part	18	18.750	1.22E-05	TNXB, LGALS1, CD109, IGF1, VTN, MMP14, CCL4, TGFB1, BGN, COL7A1, CXCL14, NPY, CXCL16, COMP, TGFBI, COL1A1, LOXL2, VNN3	85	774	12504	3.421	0.0017	8.48E-04	0.0053
5	GOTERM_BP_FAT	GO:0009611~response to wounding	12	12.500	3.34E-06	C1QA, C1QB, SLC11A1, TLR2, NPPB, F9, CCL4, TLR7, CD14, TGFB1, F2R, FCGR3	77	347	13588	6.103	0.0037	9.20E-04	0.0104
6	GOTERM_BP_FAT	GO:0048584~positive regulation of response to stimulus	9	9.375	9.03E-06	C1QA, C1QB, SLC11A1, NPY, TLR2, UNC93B1, FCER1G, RAET1B, FCGR3	77	186	13588	8.539	0.0099	0.0012	0.0141
7	GOTERM_BP_FAT	GO:0050778~positive regulation of immune response	8	8.333	1.06E-05	C1QA, C1QB, SLC11A1, TLR2, UNC93B1, FCER1G, RAET1B, FCGR3	77	136	13588	10.380	0.0116	0.0013	0.0145
8	GOTERM_BP_FAT	GO:0001817~regulation of cytokine production	8	8.333	1.22E-05	SLC11A1, TLR2, FCER1G, TLR7, CD14, RAET1B, F2R, FCGR3	77	139	13588	10.156	0.0134	0.0013	0.0170
9	GOTERM_BP_FAT	GO:0019882~antigen processing and presentation	7	7.292	8.84E-06	SLC11A1, H2-EB1, UNC93B1, FCER1G, H2-AB1, RAET1B, FCGR3	77	87	13588	14.199	0.0097	0.0014	0.0196
10	GOTERM_BP_FAT	GO:0006952~defense response	13	13.542	6.51E-06	RARRES2, TLR2, TLR7, CCL4, TGFB1, FCGR3, C1QA, C1QB, SLC11A1, NPPB, FCER1G, CD14, F2R	77	448	13588	5.121	0.0072	0.0014	0.0304
11	GOTERM_BP_FAT	GO:0002684~positive regulation of immune system process	9	9.375	1.90E-05	C1QA, C1QB, SLC11A1, TLR2, UNC93B1, FCER1G, TGFB1, RAET1B, FCGR3	77	206	13588	7.710	0.0207	0.0017	0.4742

SUPPLEMENTAL EXPERIMENTAL PROCEDURES

Animals

Strains

Experiments were performed in adult (9-10 weeks old) male C57BL/6J mice (Jackson laboratory, Maine, USA). Heterozygous TrpV1-Cre (strain #017769) and heterozygous DTA stop animals (strain #010527) were bred together to produce TrpV1 DTA animals or non DTA expressing littermates. Rag1-null (strain #2216) were bred on a C57BL/6J background and backcrossed at least 10 times. To reveal T cell infiltration in the injured DRG we bred Lck-Cre (Jax #3802) with zsGreen reporter (Rosa-CAG-LSL-ZsGreen1-WPRE) (Jax #7906).

All studies performed in USA were conducted under strict review and guidelines according to the Institutional Animal Care and Use Committee (IACUC) at Boston Children's Hospital, which meets the veterinary standards set by the American Association for Laboratory Animal Science (AALAS). The experiments were reviewed and approved by the IACUC at Boston Children's Hospital under animal protocol numbers 15-04-2928R and 16-01-3080R. All experimental procedures performed in Spain were conducted in strict accordance to European standards (European Communities Council Directive 2010/63) and after approval of the animal protocols by regional (Junta de Andalucía) and institutional (Research Ethics Committee of the University of Granada, Spain) authorities. To decrease the number of animals in this study, we used the same mice for behavioral and in vitro studies, when possible.

Spared nerve injury

Mice were anesthetized with isoflurane (2–4%) and SNI surgery performed; the tibial and common peroneal branches of the sciatic nerve were tightly ligated with a silk suture and transected distally while the sural nerve was left intact (Bourquin et al., 2006; Decosterd and Woolf, 2000). In sham-operated controls, the sciatic nerve terminal branches were exposed but not ligated. Wounds were closed and the animals returned to their cages.

Immune cell depletion or reconstitution

To deplete macrophages *in vivo*, we administered 100 µl of anionic liposome-encapsulated clodronate i.v. 24h before SNI surgery (Clophosome-ATM, FormuMax Scientific, Sunnyvale, CA), into the tail vein of mice under isofluorane anesthesia (Kobayashi et al., 2015). Liposomes devoid of clodronate were used as a control.

For *Rag1*$^{-/-}$ reconstitution experiments, $CD4^+$ and $CD8^+$ T cells were enriched from male C57BL/6J splenic and lymph node single cell suspensions using magnetically labeled anti-CD4 and anti-CD8α microbeads (Miltenyi). 5 x 10^6 $CD4^+$ and 2.5 x 10^6 $CD8^+$ T cells were injected into the tail veins of male *Rag1*$^{-/-}$ recipients. SNI surgeries were performed 16 days after transfer. Reconstitution of T cell compartments was assessed by flow cytometry on peripheral blood mononuclear cells using antibodies (Biolegend) to CD4, CD8α and B220 (to detect B cells). Flow cytometry data were collected on an LSR II analyzer (BD Biosciences) and analyzed using FlowJo software (Treestar).

Behavioral tests

Measures of mechanical and cold allodynia

A time course of tactile and cold sensitivity before and after SNI was measured in C57BL/6J mice. Animals were acclimated for two hours in test compartments (7.5 cm wide x 7.5 cm long x 15 cm high) placed on an elevated mesh-bottomed platform, to access to ventral hind paws. Two groups of mice (n=13 or 14 per group) were assayed every other day prior to and post SNI. One group was used to determine baseline 1 (BL1) then 1, 3, 5, 7, 9 and 14 days post SNI, the second was used to assay baseline 2 (BL2) then 2, 4, 6, 8, 10 and 15 days post SNI. Each group was assayed every other day to prevent animals becoming over stimulated and/or habituated to the testing. Both groups exhibited sensitivity changes that altered in a consistent fashion over the time course. Mechanical allodynia was measured using von Frey filaments (Touch-Test Sensory Evaluators; North Coast Medical Inc., Gilroy, CA) ranging from 0.07 to 2 g. Filaments were applied for 2-3 s to the sural territory of the hind paw plantar surface using the up–down paradigm (Chaplan et al., 1994). Evaluation was initiated with a 0.6-g von Frey filament. In each consecutive test, if there was no response to the filament, a stronger stimulus was then selected; if there was a positive response, a weaker one was then used. The response to the filament was considered positive if immediate licking/biting, flinching or fast withdrawal of the stimulated paw was observed.

Cold allodynia was assayed by applying a 10µl drop of acetone to the hind paw ipsilateral to the SNI injury and measuring the amount of time the animal spent flinching/licking/biting the paw in seconds. TrpV1 DTA mice were tested twice at baseline and then 7, 14 and 21 post SNI. Macrophage depleted mice were tested at baseline and on days 7, 10, 14 and 21 post SNI. Rag1 -/- and T cell addition mice were tested at baseline twice, again post T cell addition, and then 7, 14, 21 and 28 post SNI.

As mice subject to SNI develop exquisite hypersensitivity over the first week following nerve injury and this study relies on the careful determination of its onset, we took special care not to introduce any confounds in evaluating the sensitivity. For measuring tactile allodynia we took special care to reduce the effects of repeated measures that occur with repetitive von Frey stimulation, by leaving at least 30 seconds between every stimulation. When testing cold allodynia we ensured that only the acetone touched the hind paw.

All experiments were performed in at least two independent sets of mice.

Dynamic Thermal Place Aversion Test – Naïve TrpV1 DTA animals

Two thermal plates were placed directly adjacent to one another with a plastic chamber surrounding both allowing free movement between each plate (Bioseb, France). The temperature of each plate was set to continuously change by 1.05 degrees Celsius per minute. At the start of the experiment plate A was set at 4ºC (noxious cold) the alternate plate was set to 25ºC (ambient). The gradient of temperature change was equal on both plates but opposite, so as plate A's temperature rose toward 25ºC the alternate plate's temperature was reduced toward 4ºC with this half-cycle complete in 22 minutes. Once these temperatures had been reached, the direction of the temperature change for each plate was reversed, so that plate A now returned back to 4ºC and B to 25ºC to complete the cycle. Constantly moving the plate temperatures is required to prevent the animals settling in the ambient option. The time spent in each plate was automatically recorded at 30 s intervals using Ethovison XT v11.5 video-tracking software (Noldus, Netherlands). Experiments were performed in at least two independent sets of mice.

Data analysis of behavioral studies

Statistical analysis was carried out with a one-way or two-way repeated measures analysis of variance (ANOVA), followed by a Bonferroni post-hoc test in all cases. The differences between values were considered significant when the p-value was below 0.05. The data were analyzed with SigmaPlot 12.0 software (Systat Sofware Inc, CA, USA).

RNA analysis

RNA preparation

We studied DRGs collected in three biological replicates every 8 hours from the time of SNI until 24 hours post injury, and then daily until 10 days. Total RNA was extracted from naive and injured DRGs (ten ipsilateral L4/5 DRGs per sample, five mice) using Trizol reagent (Fisher Biotech) and standard methods. Total RNA quality evaluated with the Agilent Bioanalyzer (Agilent Technologies).

For RNAseq three biological replicates distinct to those collected above were assayed. Total RNA was extracted from naive and injured DRGs (six ipsilateral L4/5 DRGs per sample, three mice) using Trizol as above.

Microarray-based gene expression analysis

Total RNA (200 ng) was amplified, biotinylated, and hybridized to 40 Illumina MouseRef-8 v2.0 Expression BeadChips. Raw data were analyzed using Bioconductor packages (www.bioconductor.org).

Additional biologically independent groups of naive uninjured DRGs (n=7) were assayed to increase the accuracy of the baseline reference values. Clustering based on top variant genes was used to assess overall data coherence. The inter-array Pearson correlation across all probes between each array and all others was used to identify outliers, defined as having an average Pearson correlation >2 standard deviations away from the mean. Four outliers were excluded from the analysis, and data renormalized after outlier exclusion.

Contrast analysis of differential expression was performed using the LIMMA package (Smyth, 2005) After linear model fitting, we calculated 1) a Bayesian estimate of differential expression (moderated t-statistic) for all comparisons; and 2) an overall moderated F-statistic (F) combining the t-statistics for all the contrasts into an overall test of significance. The moderated F-statistics is similar to the ordinary F-statistic from analysis of variance except that the denominator mean squares are moderated across genes (https://www.bioconductor.org/packages/devel/bioc/vignettes/limma/inst/doc/usersguide.pdf). The threshold for statistical significance was set at $p<0.005$ for individual comparisons and at $p<0.01$ across the time course. Only transcripts significant in the moderated F-statistics were used for further analyses (1704 probes). Expression data from microarray can be found in GEO (accession number GSE102937).

RNAseq-based gene expression analysis

The samples were sequenced by the UCLA Neuroscience Genomics Core. RNA-sequencing was carried out using Nugen Ovation RNA Ultra Low Input (500 pg) + TruSeq Nano and then sequenced at 69bp paired end reads. The paired end sequencing reads were aligned to mouse genome (mm10) using aligner STAR with default parameters, read counts were obtained with HTSeq-count. Differential expression analyses were performed with software R and Bioconductor packages of edgeR and limma voom. GEO accession number (GSE102937).

Q-PCR-based gene expression analysis

Ipsilateral L4/L5 DRGs were harvested and RNA extracted by acid phenol extraction (TRIzol reagent, Invitrogen). First-stranded cDNA synthesis (1 µg of total RNA per reaction) was performed with SuperScript III Reverse Transcriptase (Invitrogen). Quantitative real-time PCR was performed using the Sybr green detection system with primer sets designed using the Primer Blast algorithm (NCBI), primer pairs were designed to span an intron whenever possible. Specific PCR product amplification was confirmed using the amplicon dissociation protocol. Transcript regulation was determined using the relative standard curve method (Applied Biosystems). Relative loading was determined before RT with RNA spectrophotometry followed by gel electrophoresis and after RT by amplification of glyceraldehyde-3-phosphate dehydrogenase. We tested the DRG expression of TrpV1, TrpM8 and TrpA1 in TrpV1 DT mice and their wild-type LM controls, and the expression of the macrophage markers CD68, Iba1 and CD163 in liposome controls- and clodronate-treated mice. Values were compared using an unpaired Student's t test using SigmaPlot 12.0 software (Systat Sofware Inc).

Bioinformatics

Weighted Gene Co-Expression Network Analysis

To facilitate identification of gene modules (groups of highly co-expressed genes), we constructed a weighted gene co-expression network (WGCNA) using the regulated transcripts. Briefly, we computed the absolute Pearson correlation coefficients between each probe and every other probe in the expression dataset; these values were used to determine the topological overlap, a measure of connection strength, or 'neighborhood sharing', in the network. This resulted in modules of highly co-expressed genes where the members of each network have high topological overlap in their temporal patterns of regulation (Horvath et al., 2006; Oldham et al., 2008; Parikshak et al., 2015). Heat maps were generated using HetMapImage tool from GenePattern software (v. 3.9.10).

Sensory Modality Expression Correlations

To correlate expression over time of genes defined as regulated with the temporal changes in behavioral hypersensitivity we used the Pearson correlation coefficient as a measure of the degree of linear dependence between transcript regulation and sensory hypersensitivity. This parameter ranges from -1 (complete inverse correlation) through zero (no correlation) to 1 (maximal direct correlation). Both direct and inverse correlation coefficients were used to define genes whose expression changes were similar to pain-like hypersensitivity changes over time.

RNAseq based Expression Correlations

To biologically validate the sensory modality results, we tested whether the transcripts within sensory modality group showed a similar regulation profile using RNAseq data from independent tissue samples. We selected all common transcripts in both platforms within each gene cluster and compared the resulting heat maps. Heat maps were generated as above.

Functional Enrichment Analyses

To initially identify functional categories heavily represented within either each gene expression cluster (from the WGCNA analysis) or behavioral sensory modality correlated transcript group (from the Pearson hypersensitivity correlated lists) we analyzed each gene list with Ingenuity Pathway Analysis (IPA) software, version 9.0 (Qiagen, USA). As a second method to determine cellular functions predominant in the pain modality correlated gene lists, we employed the Gene Ontology (GO) software (http://geneontology.org/). For the IPA based gene list / functional pathway correlations we used a Pearson cut off of 0.85 (±); for GO based gene list / gene function correlations we used a relatively less restrictive Pearson 0.75 (±) cut off. A lower threshold was used for the GO analysis because this algorithm performs better with more transcripts in the gene lists than the IPA algorithm which loses specificity at lower thresholds.

In addition to these two gene function predicting algorithms we chose to independently assay the content of each gene group (WGCNA expression cluster or Pearson behavior correlate) by comparing them to two gene expression sets from the literature. To represent DRG neurons we used a nociceptor specific gene expression set, obtained from FACS isolated Nav1.8 positive DRG neurons from the mouse (GSE46546 (Chiu et al., 2014)). Nav1.8 is expressed in about 80% of total DRG neurons, including a large proportion of C-fibers and

a smaller population of medium-sized myelinated cells, and therefore this set includes the signature of nociceptive neurons. To represent resident and infiltrating immune cells in the DRG post nerve injury we used a mouse activated macrophage expression set (GSE28621, F4/80+, CD11b+ inflammation-associated macrophages 72 hours post stimulation, from (Rosas et al., 2014)). To represent activated T cells we used a mouse Th1 polarized T cell expression set (GSE60354, DNRAR_YFP_IFNG Interferon stimulated T cells, from (Brown et al., 2015)). These leukocyte subsets represent a large proportion of the immune cells in the DRG after nerve injury (Hu and McLachlan, 2002).

Transcription factor binding site enrichment

Transcription factor binding site (TFBS) enrichment analysis was performed by scanning the canonical promoter region (1000bp upstream of the transcription start site) for the genes present in all eight clusters. Next we utilized TFBS position weight matrices (PWMs) from JASPAR (205 non-redundant and experimentally defined motifs) and TRANSFAC (2,208 redundant, manually curated database, extracted from the original scientific literature motifs) databases (Matys et al., 2003; Portales-Casamar et al., 2010) to examine the enrichment for corresponding TFBS within each cluster. For TFBS enrichment all the cluster were scanned with each PWMs using Clover algorithm (Frith et al., 2004). To compute the enrichment analysis we utilized three different background datasets (1000 bp sequences upstream of all mouse genes, mouse CpG islands and mouse chromosome 19 sequence), and the TFs were considered significant when $p<0.05$ relative to all 3 background/control datasets.

Protein-Protein Interaction (PPI) network analyses

We constructed an experimentally validated protein–protein interaction (PPI) network using all the genes present in the eight clusters. We created all possible combinations of gene pairs present in these clusters and identified all experimentally verified interaction data (in humans dataset) for their corresponding proteins in the STRING database (integration of the following databases: BIND, DIP, GRID, HPRD, IntAct, MINT, and PID) (Franceschini et al., 2013), constructing the protein network by force-directed layout using edge betweenness. The size of each node in the PPI network is determined by its corresponding protein's literature association with neuropathic pain. For that we determined the association with the following key-words: tactile allodynia, cold allodynia, neuropathic sensitivity or neuropathic pain in the PubMed database for every protein using R (http://cran.r-project.org/).

FACS

Briefly, total blood, and ipsilateral L3-5 DRGs were harvested from Liposome or Clodronate treated animals following nerve injury. For blood, red cells were lysed using red blood cell lysis buffer (Sigma). DRG's were digested in collagenase/dispase for 1hr at 37C, gently dissociated, and stained with the following antibodies (all from eBioscience, clone designations in parentheses): CD45 (30-F11), CD3 (145-2C11), CD11b (M1/70), CD11c (N418) and Siglec-F (1RNM44N). All samples were pre-incubated with anti-CD16/32 to block Fc receptors. Samples were read using a BD LSRFortessa.

T cell Labeling and Macrophage Immunostaining

On day 7 after surgery, SNI mice treated with clodronate or its vehicle were anesthetized with isoflurane 3% (Braun VetCare, Barcelona, Spain) in oxygen and transcardially perfused with 0.9% saline solution followed by 4 % paraformaldehyde with 1.5 % picric acid in 0.1 M phosphate buffer (pH 7.4). L4 ipsilateral DRGs were excised, post-fixed one hour 4 °C in the same fixative solution, cryoprotected for 48 h at 4 °C in 30% sucrose (Sigma-Aldrich, Madrid, Spain) in water, embedded in optimal cutting temperature embedding compound (O.C.T., Sakura Tissue-Tek, CA, USA) and frozen at −80 °C. Longitudinal DRG sections were serially cut in a cryostat at 15 µm and thaw-mounted onto microscope slides (Sigma-Aldrich). Slides were washed in TBST (tris-buffered saline with Tween 20 [0.1%]) and incubated in a blocking solution containing 5% normal goat serum (Jackson Immuno Research, PA, USA) in TBST for 1 hour at room temperature (RT) and then incubated at 4 °C overnight with an anti-IBA1 (1:1000, Wako, Japan) as a marker of macrophages/monocytes. Following primary antibody incubation, the tissue sections were washed and incubated for 1 h (RT) with secondary antibody solution containing goat anti-rabbit Alexa Fluor 488 (1:500, Life Technologies, Carlsbad, CA, USA). Antibody solutions were prepared in TBST with 5% normal goat serum and 0.3% Triton X-100 (Sigma-Aldrich). Slides were coverslipped with ProLong® Gold Antifade mounting medium (Molecular Probes; Oregon, USA) and visualized under an fluorescente microscope (Nikon Eclipse Ti, Nikon Instruments Inc., Melville, NY, USA) and processed with Image-J software (version 1.48, Wayne Rasband, NIH, Bethesda, MD, USA). To reveal T cell infiltration in the injured DRG we bred Lck-Cre (Jax #3802) with zsGreen reporter (Rosa-CAG-LSL-ZsGreen1-WPRE) (Jax #7906), and followed the same procedure described above but using a secondary antibody solution containing goat anti-rabbit Alexa Fluor 594 (1:500, Life Technologies, Carlsbad, CA, USA) to label the primary anti-IBA1. These animals express the strong florescent green marker in activated T cells.

SUPPLEMENTAL REFERENCES

Bourquin, A.F., Suveges, M., Pertin, M., Gilliard, N., Sardy, S., Davison, A.C., Spahn, D.R., and Decosterd, I. (2006). Assessment and analysis of mechanical allodynia-like behavior induced by spared nerve injury (SNI) in the mouse. Pain 122, 14 e11-14.

Chaplan, S.R., Bach, F.W., Pogrel, J.W., Chung, J.M., and Yaksh, T.L. (1994). Quantitative assessment of tactile allodynia in the rat paw. Journal of neuroscience methods 53, 55-63.

Franceschini, A., Szklarczyk, D., Frankild, S., Kuhn, M., Simonovic, M., Roth, A., Lin, J., Minguez, P., Bork, P., von Mering, C., and Jensen, L.J. (2013). STRING v9.1: protein-protein interaction networks, with increased coverage and integration. Nucleic acids research 41, D808-815.

Frith, M.C., Fu, Y., Yu, L., Chen, J.F., Hansen, U., and Weng, Z. (2004). Detection of functional DNA motifs via statistical over-representation. Nucleic acids research 32, 1372-1381.

Horvath, S., Zhang, B., Carlson, M., Lu, K.V., Zhu, S., Felciano, R.M., Laurance, M.F., Zhao, W., Qi, S., Chen, Z., et al. (2006). Analysis of oncogenic signaling networks in glioblastoma identifies ASPM as a molecular target. Proceedings of the National Academy of Sciences of the United States of America 103, 17402-17407.

Matys, V., Fricke, E., Geffers, R., Gossling, E., Haubrock, M., Hehl, R., Hornischer, K., Karas, D., Kel, A.E., Kel-Margoulis, O.V., et al. (2003). TRANSFAC: transcriptional regulation, from patterns to profiles. Nucleic acids research 31, 374-378.

Oldham, M.C., Konopka, G., Iwamoto, K., Langfelder, P., Kato, T., Horvath, S., and Geschwind, D.H. (2008). Functional organization of the transcriptome in human brain. Nature neuroscience 11, 1271-1282.

Portales-Casamar, E., Thongjuea, S., Kwon, A.T., Arenillas, D., Zhao, X., Valen, E., Yusuf, D., Lenhard, B., Wasserman, W.W., and Sandelin, A. (2010). JASPAR 2010: the greatly expanded open-access database of transcription factor binding profiles. Nucleic acids research 38, D105-110.